ADAPTIVE ROBUST TRACKING RBF NEURAL NETWORKS CONTROL FOR INDUSTRIAL ROBOT MINIPULATORS BASED ON BACKSTEPPING

Vu Thi Yen*

Hanoi University of Industry

*Corresponding author: havi2203@gmail.com

(Received: September 15, 2021; Accepted: February 28, 2022)

Abstract - This present study proposes a design and the analysis of the novel adaptive robust neural networks (ARNNs) based on the backstepping control method for industrial robot manipulators (IRMs). In this research, the ARNNs controller has combined the advantages of Radial Basis Function neural network (RBFNN), the robust term, and adaptive backstepping control technique without the requirement of prior knowledge. The RBFNN is used in order to approximate the unknown function to deal with external disturbances and uncertain nonlinearities. In addition, the disturbance of system is compensated by the robust Sliding Mode Control (SMC). All the parameters of ARNNs are determined by the Lyapunov stability theorem, are tuned online by an adaptive training law. Therefore, the stability, robustness, and desired tracking of the performance of ARNNs for IRMs are guaranteed.

Key words - Adaptive control; sliding mode control; neural networks; Adaptive fuzzy logic control; industrial robot

1. Introduction

In recent years, interest in designing robust tracking control for industrial robot manipulator system has been increased, and a lot of significant research attentions have been attracted. However, IRMs are multi-input multi-output non-linear systems and in the working process, they usually bear the nonlinear friction, payload variation, external disturbance, etc. in their dynamics. Hence, it is hard to design an exact controller without the knowledge of the robotic system. To solve these difficulties, many controllers for IRMs have been proposed, including PID control, adaptive control, intelligent control, SMC, backstepping control, fuzzy control and variable structureone, etc. [1-4].

In the past decade, the backstepping technique for designing an adaptive controller for nonlinear systems has been widely applied [5-8]. In [5], Chien – Wen Chung, Yaote Chang have applied this methods to deal with the regulation problems for nonlinear systems. The robustness and stability of the control system were improved by using the proposed controller. In [7], the combined advantages of SMC and the backstepping algorithm were proposed to improve the position tracking error of the 3-DOF PM spherical actuator. Here, by using the backstepping technique, the stability of the closed-loop system could be guaranteed and the disturbance of the system could be compensated by the robust term. Thus, the proposed controller could guarantee better tracking performance. In general, all investigations based on backstepping control methods in [5-8] were proposed suitable to control for nonlinear systems. However, this Backstepping design method still exits some problems such as the certain functions are “linear in the unknown parameters”, which is not satisfied in practice. Furthermore, determining and calculating the regression matrices are more acute.

Recently, many researchers have successfully applied neural network techniques to solve the problem of unmodeled and unknown dynamics for IRMs by providing online learning laws [9-13]. In [9], the authors proposed an adaptive neural network control to deal with the problem of tracking control with unknown dynamics of the robot system. The unknown model of this system was approximated by using the neural network technique and the robust term was used to compensate for the uncertainties dynamic of the robot model. In [12], the authors studied an adaptive robust controller by the neural network to overcome the problem of nonlinear MIMO systems with time delays and external disturbance. In this controller, the impact of time delays could be eliminated by using the advance of Lyapunov Krasovskii theorem and Young’s inequality, and by using the robust term to eliminate external disturbance of systems. In addition, the RBFNNs have been applied extensively to control nonlinear dynamic systems. Because of simple network structure, fast training, and better approximation capabilities. Due to the popularity of RBFNNs, many researchers have been proposed, as shown in [14-17], for example. In [14], the neural network control by RBF functions was presented to deal with the problem of the uncertainties system of biped robots. This controller was used neural networks to approximate the unknown dynamic of the biped robot. The robustness and stability of this controller for biped robot systems were guaranteed and proved based on the stability Lyapunov theorem. In [17], the authors have been studied the tracking problem of 3 – DOF robotic based on an adaptive neural network controller. This controller has been considered both output feedback and state control schemes by using two neural networks. A neural network was employed to approximate the dynamics of the robot and another neural network was used to approximate the unknown hysteresis nonlinearity.

In this studding, an adaptive robust backstepping trajectory tracking control by RBFNNs is proposed for IRMs to deal with the problem of unknown models and uncertain dynamics. By using RBFNNs to approximate the unknown function to make the adaptive backstepping control have strong robustness for the uncertain model and external disturbances of IRMs. All parameters adaptation laws are calculated based on the Lyapunov stability theorem. Furthermore, the external disturbance of IRMs can be eliminated by employing sliding mode control. Therefore, the intelligent ARNNs prove that it can be

guaranteed desired to not only track performance but also the robustness, and stability of the robot manipulators control system.

2. Problem formulation

2.1. Model of robotic manipulators

The dynamics of an n-link IRMs can be described as follows:

$$\boldsymbol{M}(\bar{q})\ddot{\bar{q}}+\boldsymbol{C}(\bar{q},\dot{\bar{q}})\dot{\bar{q}}+\boldsymbol{G}(\bar{q})+\boldsymbol{F}(\dot{\bar{q}})+\tau_d=\tau \quad (1)$$

where $\bar{q}=[q_1\ q_2\ldots q_n]\in R^{n\times 1}$ is the joint position vector, $\dot{\bar{q}}=[\dot{q}_1\ \dot{q}_2\ldots\dot{q}_n]\in R^{n\times 1}$ is the velocity vector and $\ddot{\bar{q}}=[\ddot{q}_1\ \ddot{q}_2\ldots\ddot{q}_n]\in R^{n\times 1}$ is the acceleration vector.

$M(\bar{q})$ is the $n\times n$ symmetric inertial Matrix. $\boldsymbol{C}(\bar{q},\dot{\bar{q}})$ is the $n\times n$ Coriolis vector and Centripetal forces. $\boldsymbol{G}(\bar{q})$ is an $n\times 1$ vector containing Gravity forces and torques. $F(\bar{q})$ is an $n\times 1$ vector of friction term. τ_d is an $n\times 1$ unknown disturbances vector and τ is an $n\times 1$ vector of control input torque. For designing controller, the robot dynamics (1) has the following fundamental properties:

Property 1: $\boldsymbol{M}(q)$ is the $n\times n$ symmetric inertial Matrix and bounded:

$$\vartheta_1 x^2\le x^T\boldsymbol{M}(\bar{q})x\le\vartheta_2 x^2,\forall x\in R^{n\times 1} \quad (2)$$

with ϑ_1 and ϑ_2 are positive constants.

Property 2: $\left[\dot{\boldsymbol{M}}(\bar{q})-2\boldsymbol{C}(\bar{q},\dot{\bar{q}})\right]$ is skew symmetric matrix and satisfies:

$$x^T\left[\dot{\boldsymbol{M}}(\bar{q})(\bar{q})-2\boldsymbol{C}(\bar{q},\dot{\bar{q}})\right]x=0 \quad (3)$$

Property 3: $\boldsymbol{C}(\bar{q},\dot{\bar{q}})\dot{\bar{q}}$, $\boldsymbol{G}(\bar{q})$ and $\boldsymbol{F}(\dot{\bar{q}})$ are satisfied:

$$\boldsymbol{C}(\bar{q},\dot{\bar{q}})\dot{\bar{q}}\le C_k\dot{\bar{q}}^2,\boldsymbol{G}(\bar{q})\le G_k,\boldsymbol{F}(\dot{\bar{q}})\le F_k \quad (4)$$

where M_k, G_k, F_k are positive constants.

2.2. Backstepping controller

The conventional Backstepping controller for the dynamic of the IRMs is described as follows:

Step 1: the tracking error vector $\bar{z}_{q1}(t)$ and derivative of $\bar{z}_{q1}(t)$ are define as the follows:

$$\bar{z}_{q1}(t)=\bar{q}_d-\bar{q}\ and\ \dot{\bar{z}}_{q1}(t)=\dot{\bar{q}}_d-\dot{\bar{q}} \quad (5)$$

By using $\dot{\bar{q}}$ as the first virtual control input. Define an intermediate function as:

$$\alpha_{q1}(t)=\dot{\bar{q}}_d+\lambda_{q1}\bar{z}_{q1}\ \text{and}\ \dot{\alpha}_{q1}(t)=\ddot{\bar{q}}_d+\lambda_{q1}\dot{\bar{z}}_{q1}\ \text{with}\ \lambda_{q1}>0 \quad (6)$$

Consider the first following Lyapunov function candidate L_1 as:

$$L_{q1}(\bar{z}_{q1}(t))=\frac{1}{2}\bar{z}_{q1}^T\bar{z}_{q1} \quad (7)$$

The tracking error vector $\bar{Z}_{q2}(t)$ is define as the follows:

$$\bar{z}_{q2}(t)=\alpha_{q1}(t)-\dot{\bar{q}}=\dot{\bar{z}}_{q1}+\lambda_{q1}\bar{z}_{q1} \quad (8)$$

The derivative of $L_{q1}(\bar{z}_{q1}(t))$ is:

$$\dot{L}_{q1}(\bar{z}_{q1}(t))=\bar{z}_{q1}^T\dot{\bar{z}}_{q1}=\bar{z}_{q1}^T(\bar{z}_{q2}(t)-\lambda_{q1}\bar{z}_{q1}) \quad (9)$$

Step 2: the derivative of $\bar{z}_{q2}(t)$ along to time, we have

$$\dot{\bar{z}}_{q2}(t)=\dot{\alpha}_{q1}(t)-\ddot{\bar{q}} \quad (10)$$

where $\ddot{\bar{q}}$ used as the second virtual control input.

Substituting (5, 6, 8, 10) into (1), we have:

$$\boldsymbol{M}\dot{\bar{z}}_{q2}=\boldsymbol{M}\dot{\alpha}_{q1}+\boldsymbol{C}\alpha_{q1}-\boldsymbol{C}\bar{z}_{q2}+\boldsymbol{G}+\boldsymbol{F}+\tau_d-\tau \quad (11)$$

Consider the second Lyapunov function L_2 as follows:

$$L_{q2}(\bar{z}_{q1},\bar{z}_{q2})=L_{q1}(\bar{z}_{q1}(t))+\frac{1}{2}\bar{z}_{q2}^T\boldsymbol{M}\bar{z}_{q2} \quad (12)$$

The derivative of $L_{q2}(\bar{z}_{q1}(t),\bar{z}_{q2}(t))$ is:

$$\dot{L}_{q2}=\bar{z}_{q1}^T(\bar{z}_{q2}(t)-\lambda_{q1}\bar{z}_{q1})+\frac{1}{2}\bar{z}_{q2}^T\dot{\boldsymbol{M}}\bar{z}_{q2}+\bar{z}_{q2}^T\boldsymbol{M}\dot{\bar{z}}_{q2} \quad (13)$$

Substituting (11) into (13) and use Property *2*, we have:

$$\dot{L}_{q2}=\bar{z}_{q1}^T(\bar{z}_{q2}(t)-\lambda_{q1}\bar{z}_{q1})+\frac{1}{2}\bar{z}_{q2}^T\dot{\boldsymbol{M}}\bar{z}_{q2}+\bar{z}_{q2}^T(\boldsymbol{M}\dot{\alpha}_{q1}+\boldsymbol{C}\alpha_{q1}-\boldsymbol{C}\bar{z}_{q2}+\boldsymbol{G}+\boldsymbol{F}+\tau_d-\tau) \quad (14)$$

$$\dot{L}_{q2}=\bar{z}_{q1}^T\bar{z}_{q2}(t)-\bar{z}_{q1}^T\lambda_{q1}\bar{z}_{q1}+\frac{1}{2}\bar{z}_{q2}^T(\dot{\boldsymbol{M}}-2\boldsymbol{C})\bar{z}_{q2}+\bar{z}_{q2}^T(y+\tau_d-\tau) \quad (15)$$

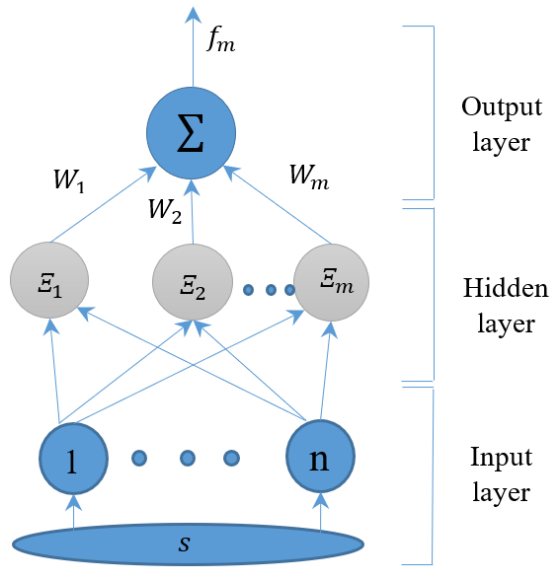

Figure 1. *Structure of RBFNN*

$$\dot{L}_{\Sigma 2}=\bar{z}_{q1}^T\bar{z}_{q2}(t)-\bar{z}_{q1}^T\lambda_{q1}\bar{z}_{q1}+\bar{z}_{q2}^T(y+\tau_d-\tau) \quad (16)$$

With: $y=\boldsymbol{M}\dot{\alpha}_{q1}+\boldsymbol{C}\alpha_{q1}+G+F$ (17)

To continue our design, the adaptive control law is presented as:

$$\tau = y + \lambda_{q2}\bar{z}_{q2} + \bar{z}_{q1} + \tau_{SMC} \tag{18}$$

with $\lambda_{q2} > 0$

Substituting (16) into (14), we have:

$$\dot{L}_{q2} = -\bar{z}_{q1}^T\lambda_{q1}\bar{z}_{q1} - \bar{z}_{q2}^T\lambda_{q2}\bar{z}_{q2} \le 0 \tag{19}$$

Since (19), $\dot{L}_{q2} < 0$, so

$$\dot{L}_{q2}\left(\bar{z}_{q1}(t), \bar{z}_{q2}(t)\right) \le \dot{L}_{q2}\left(\bar{z}_{q1}(0), \bar{z}_{q2}(0)\right).$$

If $\bar{z}_{q1}(t), \bar{z}_{q2}(t)$ is bounded with $t > 0$. By defining

$$\epsilon(t) = -\bar{z}_{q1}^T\lambda_{q1}\bar{z}_{q1} - \bar{z}_{q2}^T\lambda_{q2}\bar{z}_{q2}$$

so $\epsilon(t) \le -\dot{L}_{q2}\left(\bar{z}_{q1}(t), \bar{z}_{q2}(t)\right)$ and integrate the $\epsilon(t)$ with respect to time as follows:

$$\int_0^t \epsilon(\zeta)d\zeta \le -L_{q2}\left(\bar{z}_{q1}(t), \bar{z}_{q2}(t)\right) + L_{q2}\left(\bar{Z}_{q1}(0), \bar{Z}_{q2}(0)\right) \tag{20}$$

Because $L_{q2}\left(\bar{z}_{q1}(0), \bar{z}_{q2}(0)\right)$ is a bounded function, and $L_{q2}\left(\bar{z}_{q1}(t), \bar{z}_{q2}(t)\right)$ is and non-increasing bounded, we have:

$$\lim_{t\to\infty}\int_0^t \epsilon(\zeta)d\zeta < \infty \tag{21}$$

According to Barbalat's Lemma [18], when $\dot{\epsilon}(t)$ is bounded function. It can be shown that $\lim_{t\to\infty}\int_0^t \epsilon(t)dt = 0$. From this result, we see that, $\bar{z}_{q1}(t), \bar{z}_{q2}(t)$ will converge to zero when $t \to \infty$ and the global stability of the control system for IRMs is guaranteed.

2.3. The Architecture of RBFNN

The architecture of RBFNN is shown in Fig.1, which includes three-layer: Layer 1 (Input layer), Layer 2 (Hidden layer), and Layer 3 (Output layer).

The output of hidden layer is calculated as follows:

$$\Xi_j(s) = exp[-(s-c_j)^2/(2d_j^2)]; j = 1,2,..,m \tag{22}$$

where m is the number of hidden nodes, $c_j = c_{j1}, \dots, c_{jn}$ is the center vector of neural net j, d_j notes the standard deviation of the jth radial basis function, $d = [d_1, \dots, d_m]^T$, and Ξ_j is Gaussian activation function for neural net j.

According to [19], the output values of ideal RBFNNs determined as:

$$f(\bar{s}) = \boldsymbol{W}^T\Xi(\bar{s}) + \Gamma \tag{23}$$

Here, $\boldsymbol{W}$ is ideal optimum weight values of RBFNNs. Γ is modeling error of f

The approximate value of the output RBF is designed as:

$$\hat{f}(s) = \hat{\boldsymbol{W}}^T\Xi(s) \tag{24}$$

Assume that $\boldsymbol{M}(\bar{q}), \boldsymbol{C}(\bar{q}, \dot{\bar{q}}), \boldsymbol{G}(\bar{q})$ and $\boldsymbol{F}(\dot{\bar{q}})$ are the output values of ideal RBFNNs and determined, respectively as:

$$\boldsymbol{M}(\bar{q}) = \boldsymbol{M}_R(\bar{q}) + \Gamma_M = \boldsymbol{W}_M^T * \Xi_M(\bar{q}) + \Gamma_M \tag{25}$$

$$\boldsymbol{C}(\bar{q}, \dot{\bar{q}}) = \boldsymbol{C}_R(\bar{q}, \dot{\bar{q}}) + \Gamma_C = \boldsymbol{W}_C^T * \Xi_C(\bar{q}, \dot{\bar{q}}) + \Gamma_C \tag{26}$$

$$\boldsymbol{G}(\bar{q}) = \boldsymbol{G}_R(\bar{q}) + \Gamma_G = \boldsymbol{W}_G^T * \Xi_G(\bar{q}) + \Gamma_G \tag{27}$$

$$\boldsymbol{F}(\dot{\bar{q}}) = \boldsymbol{F}_R(\dot{\bar{q}}) + \Gamma_F = \boldsymbol{W}_F^T * \Xi_F(\dot{\bar{q}}) + \Gamma_F \tag{28}$$

with $\boldsymbol{W}_M, \boldsymbol{W}_C, \boldsymbol{W}_G$, and $\boldsymbol{W}_F$ are ideal optimum weight values of RBF; Ξ_M, Ξ_C, Ξ_G, and Ξ_F are outputs of hiden layer, $\Gamma_M, \Gamma_C, \Gamma_G$ and Γ_F are modeling errors of $\boldsymbol{M}(\bar{q}), \boldsymbol{C}(\bar{q}, \dot{\bar{q}}), \boldsymbol{G}(\bar{q})$ and $\boldsymbol{F}(\dot{\bar{q}})$, respectively. $\hat{\boldsymbol{M}}_R(\bar{q}), \hat{\boldsymbol{C}}_R(\bar{q}, \dot{\bar{q}}), \hat{G}_R(\bar{q})$ and $\hat{\boldsymbol{F}}_R(\dot{\bar{q}})$ are the estimated values of the $\boldsymbol{M}_R(\bar{q}), \boldsymbol{C}_R(\bar{q}, \dot{\bar{q}}), \boldsymbol{G}_R(\bar{q}), \boldsymbol{F}_R(\dot{\bar{q}})$, respectively, and they are described as follows:

$$\hat{\boldsymbol{M}}_R(\bar{q}) = \hat{\boldsymbol{W}}_M^T * \Xi_M(\bar{q}) \tag{29}$$

$$\hat{\boldsymbol{C}}_R(\bar{q}, \dot{\bar{q}}) = \hat{\boldsymbol{W}}_C^T * \Xi_C(\bar{q}, \dot{\bar{q}}) \tag{30}$$

$$\hat{\boldsymbol{G}}_R(\bar{q}) = \hat{\boldsymbol{W}}_G^T * \Xi_G(\bar{q}) \tag{31}$$

$$\hat{\boldsymbol{F}}_R(\dot{\bar{q}}) = \hat{\boldsymbol{W}}_F^T * \Xi_F(\dot{\bar{q}}) \tag{32}$$

in which $\widehat{\boldsymbol{W}}_M$, $\widehat{\boldsymbol{W}}_C, \widehat{\boldsymbol{W}}_G$, and $\widehat{\boldsymbol{W}}_F$ are estimates of $\boldsymbol{W}_M, \boldsymbol{W}_C, \boldsymbol{W}_G$ and $\boldsymbol{W}_F$, respectively.

3. Design controller and stability analysis

Here, we proposed an intelligent controller which combines adaptive neural networks control and the Backstepping technique to suppress the effects of the uncertainties and approximation errors. Thus, the unknown functions of the robot manipulator control system are estimated, and stability can be guaranteed. The block diagram of ARNNs is described in Figure 2.

The ARNNs control law is presented as:

$$\tau = \hat{y} + \lambda_{q2}\bar{z}_{q2} + \bar{z}_{q1} + \hat{\tau}_{SMC} \tag{33}$$

where $\hat{\tau}_{SMC}$ is a SMC robust term, and $\hat{y}$ is the approximation of the function y

Substituting (6), and (25-28) into (17), equation (17) can be rewritten as follows:

$$\begin{aligned} y &= \left(\boldsymbol{W}_M^T * \Xi_M(\bar{q}) + \Gamma_M\right)\left(\ddot{\bar{q}}_d + \lambda_{q1}\dot{\bar{z}}_{q1}\right) + \boldsymbol{W}_F^T * \Xi_F(\dot{\bar{q}}) + \Gamma_F \\ &\quad + \left(\boldsymbol{W}_C^T * \Xi_C(\bar{q}, \dot{\bar{q}}) + \Gamma_C\right)\left(\dot{\bar{q}}_d + \lambda_{q1}\bar{z}_{q1}\right) + \boldsymbol{W}_G^T * \Xi_G(\bar{q}) + \Gamma_G \\ y &= \boldsymbol{W}_M^T * \Xi_M(\bar{q})\left(\ddot{\bar{q}}_d + \lambda_{q1}\dot{\bar{z}}_{q1}\right) + \Gamma_C\left(\dot{\bar{q}}_d + \lambda_{q1}\bar{z}_{q1}\right) \\ &\quad + \boldsymbol{W}_G^T * \Xi_G(\bar{q}) + W_F^T * \Xi_F(\dot{\bar{q}}) + \Gamma_M\left(\ddot{\bar{q}}_d + \lambda_{q1}\dot{\bar{z}}_{q1}\right) \\ &\quad + \boldsymbol{W}_C^T * \Xi_C(\bar{q}, \dot{\bar{q}})\left(\dot{\bar{q}}_d + \lambda_{q1}\bar{z}_{q1}\right) + \Gamma_G + \Gamma_F \\ y &= \boldsymbol{W}_M^T * \Xi_M(\bar{q})\left(\ddot{\bar{q}}_d + \lambda_{q1}\dot{\bar{z}}_{q1}\right) + \boldsymbol{W}_G^T * \Xi_G(\bar{q}) \\ &\quad + \boldsymbol{W}_C^T * \Xi_C(\bar{q}, \dot{\bar{q}})\left(\dot{\bar{q}}_d + \lambda_{q1}\bar{z}_{q1}\right) + \boldsymbol{W}_F^T * \Xi_F(\dot{\bar{q}}) + \Gamma \end{aligned} \tag{34}$$

where $\Gamma = \Gamma_M\left(\ddot{\bar{q}}_d + \lambda_{q1}\dot{\bar{z}}_{q1}\right) + \Gamma_C\left(\dot{\bar{q}}_d + \lambda_{q1}\bar{z}_{q1}\right) + \Gamma_G + \Gamma_F$

The approximation of y is define as:

$$\hat{y} = \hat{\boldsymbol{M}}\dot{\alpha}_{q1} + \hat{\boldsymbol{C}}\alpha_{q1} + \hat{\boldsymbol{G}} + \hat{\boldsymbol{F}} \tag{35}$$

By using Eq (6), and Eqs (29-32), Eq (36) could be rewritten as follows:

$$\begin{aligned}\hat{y} = {} & \hat{\boldsymbol{W}}_M^T * \Xi_M(\bar{q})\left(\ddot{\bar{q}}_d + \lambda_{q1}\dot{\bar{z}}_{q1}\right) + \hat{\boldsymbol{W}}_G^T * \Xi_G(\bar{q}) \\ & + \hat{\boldsymbol{W}}_C^T * \Xi_C(\bar{q},\dot{\bar{q}})\left(\dot{\bar{q}}_d + \lambda_{q1}\bar{z}_{q1}\right) + \hat{\boldsymbol{W}}_F^T * \Xi_F(\dot{\bar{q}})\end{aligned} \tag{36}$$

The robust term is signed as follows:

$$\begin{aligned}\hat{\tau}_{SMC} = {} & \frac{\bar{z}_{q2}}{\bar{z}_{q2}}\left(\frac{\eta_M \boldsymbol{W}_M^2}{4} + \frac{\eta_C \boldsymbol{W}_C^2}{4} + \frac{\eta_G \boldsymbol{W}_G^2}{4} + \frac{\eta_F \boldsymbol{W}_F^2}{4}\right) \\ & + \eta_P sgn(\bar{z}_{q2}) = \frac{\bar{z}_{q2}}{\bar{z}_{q2}}\xi + \eta_P sgn(\bar{z}_{q2})\end{aligned} \tag{37}$$

where: $\xi = \frac{\eta_M \boldsymbol{W}_M^2}{4} + \frac{\eta_C \boldsymbol{W}_C^2}{4} + \frac{\eta_G \boldsymbol{W}_G^2}{4} + \frac{\eta_F \boldsymbol{W}_F^2}{4}$; $\eta_P \geq \|\Gamma + \tau_d\|$

By the above analysis, the online training laws of ARNNs controller are chosen as:

$$\begin{cases}\dot{\hat{\boldsymbol{W}}}_M = k_M \Xi_M(\bar{q})\left(\ddot{\bar{q}}_d + \lambda_{q1}\dot{\bar{z}}_{q1}\right)\bar{z}_{q2}^T - \eta_M k_M \bar{z}_{q2}\hat{\boldsymbol{W}}_M \\ \dot{\hat{\boldsymbol{W}}}_C = k_C \Xi_C(\bar{q},\dot{\bar{q}})\left(\dot{\bar{q}}_d + \lambda_{q1}\bar{z}_{q1}\right)\bar{z}_{q2}^T - \eta_C k_C \bar{z}_{q2}\hat{\boldsymbol{W}}_C \\ \dot{\hat{\boldsymbol{W}}}_G = k_G \Xi_G(\bar{q})\bar{z}_{q2}^T - \eta_G k_G \bar{z}_{q2}\hat{\boldsymbol{W}}_G \\ \dot{\hat{\boldsymbol{W}}}_F = k_F \Xi_F(\dot{\bar{q}})\bar{z}_{q2}^T - \eta_F k_F \bar{z}_{q2}\hat{\boldsymbol{W}}_F\end{cases} \tag{38}$$

where $k_M, k_C, k_G, k_F, , \eta_M, \eta_C, \eta_G, \eta_F$ are the positive and diagonal constant matrices.

Theorem: Consider the dynamic of IRMs model in (1), the online training laws are signed in (39), and a robust term τ_{SMC} is given by (38), then the approximation tracking error and all parameters of the proposed controller are bounded, and $\bar{z}_{q1}, \bar{z}_{q2} \to 0$.

The Lyapunov function candidate is chosen as follows:

$$\begin{aligned}L(t) = {} & \frac{1}{2}\bar{z}_{q1}^T\bar{z}_{q1} + \frac{1}{2}\bar{z}_{q2}^T\boldsymbol{M}\bar{z}_{q2} + \frac{1}{2}\Big(tr\left(\tilde{\boldsymbol{W}}_M^T k_M^{-1}\tilde{\boldsymbol{W}}_M\right) \\ & + tr\left(\tilde{\boldsymbol{W}}_C^T k_C^{-1}\tilde{\boldsymbol{W}}_C\right) + tr\left(\tilde{\boldsymbol{W}}_G^T k_G^{-1}\tilde{\boldsymbol{W}}_G\right) + tr\left(\tilde{\boldsymbol{W}}_F^T k_F^{-1}\tilde{\boldsymbol{W}}_F\right)\Big)\end{aligned} \tag{39}$$

where $\tilde{\boldsymbol{W}}_M = \boldsymbol{W}_M - \hat{\boldsymbol{W}}_M$, $\tilde{\boldsymbol{W}}_C = \boldsymbol{W}_C - \hat{\boldsymbol{W}}_C$, $\tilde{\boldsymbol{W}}_G = \boldsymbol{W}_G - \hat{\boldsymbol{W}}_G$, $\tilde{\boldsymbol{W}}_F = \boldsymbol{W}_F - \hat{\boldsymbol{W}}_F$

The derivative of $L(t)$ along to time is:

$$\begin{aligned}\dot{L}(t) = {} & \bar{z}_{q1}^T\dot{\bar{z}}_{q1} + \frac{1}{2}\bar{z}_{q2}^T\dot{\boldsymbol{M}}\bar{z}_{q2} + \bar{z}_{q2}^T\boldsymbol{M}\dot{\bar{z}}_{q2} + tr\left(\tilde{\boldsymbol{W}}_M^T k_M^{-1}\dot{\tilde{\boldsymbol{W}}}_M\right) \\ & + tr\left(\tilde{\boldsymbol{W}}_C^T k_C^{-1}\dot{\tilde{\boldsymbol{W}}}_C\right) + tr\left(\tilde{\boldsymbol{W}}_G^T k_G^{-1}\dot{\tilde{\boldsymbol{W}}}_G\right) + tr\left(\tilde{\boldsymbol{W}}_F^T k_F^{-1}\dot{\tilde{\boldsymbol{W}}}_F\right)\end{aligned} \tag{40}$$

Substituting (11) and use Property 2 into (41), we have:

$$\begin{aligned}\dot{L}(t) = {} & \bar{z}_{q1}^T\bar{z}_{q2}(t) - \bar{z}_{q1}^T\lambda_{q1}\bar{z}_{q1} + \bar{z}_{q2}^T\left(y + \tau_d - \tau\right) \\ & + tr\left(\tilde{\boldsymbol{W}}_M^T k_M^{-1}\dot{\tilde{\boldsymbol{W}}}_M\right) + tr\left(\tilde{\boldsymbol{W}}_C^T k_C^{-1}\dot{\tilde{\boldsymbol{W}}}_C\right) \\ & + tr\left(\tilde{\boldsymbol{W}}_G^T k_G^{-1}\dot{\tilde{\boldsymbol{W}}}_G\right) + tr\left(\tilde{\boldsymbol{W}}_F^T k_F^{-1}\dot{\tilde{\boldsymbol{W}}}_F\right)\end{aligned} \tag{41}$$

Substituting (34), (35), (37), (39), (42), could be rewritten as follows:

$$\begin{aligned}\dot{L}(t) = {} & -\bar{z}_{q1}^T\lambda_{q1}\bar{z}_{q1} - \bar{z}_{q2}^T\lambda_{q2}\bar{z}_{q2} + \bar{z}_{q2}^T\left[\tilde{\boldsymbol{W}}_M^T * \Xi_M(\bar{q})\right]\left(\ddot{\bar{q}}_d + \lambda_{q1}\dot{\bar{z}}_{q1}\right) \\ & + \bar{z}_{q2}^T\left[\tilde{\boldsymbol{W}}_C^T * \Xi_C(\bar{q},\dot{\bar{q}})\right]\left(\dot{\bar{q}}_d + \lambda_{q1}\bar{z}_{q1}\right) \\ & + \bar{z}_{q2}^T\left[\tilde{\boldsymbol{W}}_G^T * \Xi_G(\bar{q})\right] + \bar{z}_{q2}^T\left[\tilde{\boldsymbol{W}}_F^T * \Xi_F(\dot{\bar{q}})\right] \\ & + \bar{z}_{q2}^T\left(\Gamma + \tau_d\right) - \bar{z}_{q2}^T\hat{\tau}_{SMC} - tr\left(\tilde{\boldsymbol{W}}_M^T k_M^{-1}\dot{\tilde{\boldsymbol{W}}}_M\right) - tr\left(\tilde{\boldsymbol{W}}_C^T k_C^{-1}\dot{\tilde{\boldsymbol{W}}}_C\right) \\ & - tr\left(\tilde{\boldsymbol{W}}_G^T k_G^{-1}\dot{\tilde{\boldsymbol{W}}}_G\right) - tr\left(\tilde{\boldsymbol{W}}_F^T k_F^{-1}\dot{\tilde{\boldsymbol{W}}}_F\right)\end{aligned}$$

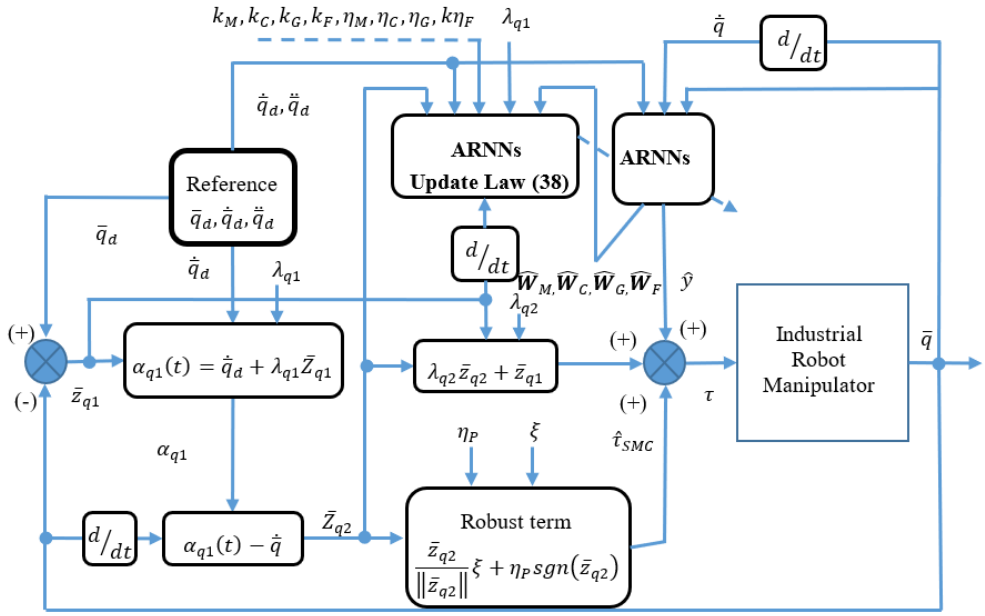

Figure 2. *The block diagram of ARNNs*

$$\begin{aligned}\dot{L}(t) = {} & -\bar{z}_{q1}^T\lambda_{q1}\bar{z}_{q1} - \bar{z}_{q2}^T\lambda_{q2}\bar{z}_{q2} + \bar{z}_{q2}^T\left(\Gamma + \tau_d\right) \\ & + \eta_C\bar{z}_{q2}\,tr\tilde{\boldsymbol{W}}_C^T\left(\boldsymbol{W}_C - \tilde{\boldsymbol{W}}_C\right) + \eta_G\bar{z}_{q2}\,tr\tilde{\boldsymbol{W}}_G^T\left(\boldsymbol{W}_G - \tilde{\boldsymbol{W}}_G\right) \\ & + \eta_F\bar{z}_{q2}\,tr\tilde{\boldsymbol{W}}_F^T\left(\boldsymbol{W}_F - \tilde{\boldsymbol{W}}_F\right) + \eta_M\bar{z}_{q2}\,tr\tilde{\boldsymbol{W}}_M^T\left(\boldsymbol{W}_M - \tilde{\boldsymbol{W}}_M\right) \\ & - \bar{z}_{q2}^T\hat{\tau}_{SMC}\end{aligned} \tag{42}$$

By using

$$tr\tilde{\boldsymbol{W}}^T\left(\boldsymbol{W} - \tilde{\boldsymbol{W}}\right) = \left(\tilde{\boldsymbol{W}}, \boldsymbol{W}\right) - \left\|\tilde{\boldsymbol{W}}\right\|^2 \leq \left\|\tilde{\boldsymbol{W}}\right\|\|\boldsymbol{W}\| - \left\|\tilde{\boldsymbol{W}}\right\|^2$$

and substituting (38) into the inequality (43) could be rewritten as follows:

$$\dot{L}(t) \le -\bar{z}_{q1}^T\lambda_{q1}\bar{z}_{q1} - \bar{z}_{q2}^T\lambda_{q2}\bar{z}_{q2} + \bar{z}_{q2}{}^T(\Gamma+\tau_d) + \eta_M\left\|\bar{z}_{q2}\right\|\left(\left\|\tilde{W}_M\right\|\left\|W_M\right\| - \left\|\tilde{W}_M\right\|^2\right) - \bar{z}_{q2}^T\frac{\bar{z}_{q2}}{\left\|\bar{z}_{q2}\right\|}\xi + \eta_C\left\|\bar{z}_{q2}\right\|\left(\left\|\tilde{W}_C\right\|\left\|W_C\right\| - \left\|\tilde{W}_C\right\|^2\right) + \eta_G\left\|\bar{z}_{q2}\right\|\left(\left\|\tilde{W}_G\right\|\left\|W_G\right\| - \left\|\tilde{W}_G\right\|^2\right) + \eta_F\left\|\bar{z}_{q2}\right\|\left(\left\|\tilde{W}_F\right\|\left\|W_F\right\| - \left\|\tilde{W}_F\right\|^2\right) - \bar{z}_{q2}^T\eta_P sgn\left(\bar{z}_{q2}\right) \quad (42)$$

$$\dot{L}(t) \le -\bar{z}_{q1}^T\lambda_{q1}\bar{z}_{q1} - \bar{z}_{q2}^T\lambda_{q2}\bar{z}_{q2} - \eta_M\left\|\bar{z}_{q2}\right\|\left(\frac{W_M}{2} - \left\|\tilde{W}_M\right\|\right)^2 - \eta_C\left\|\bar{z}_{q2}\right\|\left(\frac{W_C}{2} - \left\|\tilde{W}_C\right\|\right)^2 - \eta_G\left\|\bar{z}_{q2}\right\|\left(\frac{W_G}{2} - \left\|\tilde{W}_G\right\|\right)^2 - \eta_F\left\|\bar{z}_{q2}\right\|\left(\frac{W_F}{2} - \left\|\tilde{W}_F\right\|\right)^2 \quad (43)$$

$$\dot{L}(t) \le -\bar{z}_{q1}^T\lambda_{q1}\bar{z}_{q1} - \bar{z}_{q2}^T\lambda_{q2}\bar{z}_{q2} \quad (44)$$

From (45), $\dot{L}\left(\bar{z}_{q1}(t),\bar{z}_{q2}(t),\tilde{W}_M,\tilde{W}_C,\tilde{W}_G,\tilde{W}_F\right) \le 0$, $\dot{L}\left(\bar{z}_{q1}(t),\bar{z}_{q2}(t),\tilde{W}_M,\tilde{W}_C,\tilde{W}_G,\tilde{W}_F\right)$ is a negative semidefinite function, $\dot{L}\left(\bar{z}_{q1}(t),\bar{z}_{q2}(t),\tilde{W}_M,\tilde{W}_C,\tilde{W}_G,\tilde{W}_F\right) \le \dot{L}\left(\bar{z}_{q1}(0),\bar{z}_{q2}(0),\tilde{W}_M,\tilde{W}_C,\tilde{W}_G,\tilde{W}_F\right)$.

If $\bar{z}_{q1}(t),\bar{z}_{q2}(t),\tilde{W}_M,\tilde{W}_C,\tilde{W}_G,\tilde{W}_F$ are bounded with $t > 0$. By defining $\epsilon_L(t) = -\bar{z}_{q1}^T\lambda_{q1}\bar{z}_{q1} - \bar{z}_{q2}^T\lambda_{q2}\bar{z}_{q2}$

So $\epsilon_L(t) \le -\dot{L}(\bar{z}_{q1}(t),\bar{z}_{q2}(t),\tilde{W}_M,\tilde{W}_C,\tilde{W}_G,\tilde{W}_F)$

and integrate the $\epsilon_L(t)$ with respect to time as follows:

$$\int_0^t \epsilon_L(\zeta)d\zeta \le -L(\bar{z}_{q1}(t),\bar{z}_{q2}(t),\tilde{W}_M,\tilde{W}_C,\tilde{W}_G,\tilde{W}_F) + L(\bar{z}_{q1}(0),\bar{z}_{q2}(0),\tilde{W}_M,\tilde{W}_C,\tilde{W}_G,\tilde{W}_F) \quad (45)$$

Because $L(\bar{z}_{q1}(0),\bar{z}_{q2}(0),\tilde{W}_M,\tilde{W}_C,\tilde{W}_G,\tilde{W}_F)$ is a bounded function, and $L\left(\bar{z}_{q1}(t),\bar{z}_{q2}(t),\tilde{W}_M,\tilde{W}_C,\tilde{W}_G,\tilde{W}_F\right)$ is non-increasing and bounded, we have

$$\lim_{t\to\infty}\int_0^t \epsilon_L(\zeta)d\zeta < \infty \quad (46)$$

According to Barbalat's Lemma [18], when $\dot{\epsilon}_L(t)$ is bounded function. So $\lim_{t\to\infty}\int_0^t \epsilon_L(t)dt = 0$. From this result we see that, $\bar{z}_{q1}(t),\bar{z}_{q2}(t)$ will converge to zero when $t \to \infty$ and the global stability of the control system for IRMs is guaranteed.

4. Simulation results

Here, a three-link IRMs is applied to confirm the efficiency of the suggested control method based on ARNNs for illustrative purposes. The detailed system parameters of three-link IRMs model (Figure 3) are given as following:

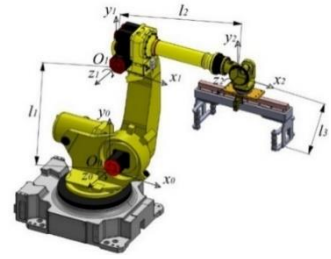

Figure 3. *The model of three-joint IRMs*

$$\boldsymbol{M} = \begin{bmatrix} M_{11} & M_{12} & M_{13} \\ M_{21} & M_{22} & M_{23} \\ M_{31} & M_{32} & M_{33} \end{bmatrix}; \boldsymbol{C} = \begin{bmatrix} C_{11} & C_{12} & C_{13} \\ C_{21} & C_{22} & C_{23} \\ C_{31} & C_{32} & C_{33} \end{bmatrix}; \boldsymbol{G} = \begin{bmatrix} G_1 \\ G_2 \\ G_3 \end{bmatrix}$$

$$M_{11} = p_2\left(l_1 + \tfrac{1}{2}l_2\cos(q_2)\right)^2 + \tfrac{1}{3}p_1l_1^2 + \tfrac{1}{2}l_2(l_1 + l_3\cos(q_2+q_3) + l_2\cos(q_2{}^2))$$

$$M_{12} = \tfrac{1}{4}p_2l_2^2 + \tfrac{1}{12}p_1l_3^2 + \tfrac{1}{4}p_3l_2^2 + \tfrac{1}{12}p_1l_3^2\cos(q_2+q_3)^2 + \tfrac{1}{12}p_1l_2^2\cos(q_2{}^2) + p_3l_1l_3\cos(q_2+q_3) + 2p_3l_2l_3\cos(q_3)$$

$$M_{23} = M_{32} = \tfrac{1}{12}p_1l_3^2 + \tfrac{1}{4}p_3l_2l_3\cos(q_3)$$

$$M_{33} = \left(\tfrac{1}{12}p_1 + \tfrac{1}{4}p_3\right)l_3^2$$

$$M_{12} = M_{13} = M_{21} = M_{31} = 0$$

$$C_{11} = -2(p_2+p_3)l_1l_2\sin(q_2)\dot{q}_2 - 2p_3l_2l_3\sin(q_3)\dot{q}_3 - 2p_3l_1l_3\sin(q_2+q_3)(\dot{q}_2+\dot{q}_3)$$

$$C_{12} = -(p_2+p_3)l_1l_2\sin(q_2)\dot{q}_2 - p_3l_1l_3\sin(q_2+q_3)(\dot{q}_2) - 2p_3l_2l_3\sin(q_3)\dot{q}_3 - 2p_3l_1l_3\sin(q_2+q_3)\dot{q}_3$$

$$C_{13} = -p_3l_2l_3\sin(q_3)\dot{q}_3 - p_3l_1l_3\sin(q_2+q_3)\dot{q}_3$$

$$C_{21} = -(p_2+p_3)l_1l_2\sin(q_2)\dot{q}_2 - p_3l_1l_3\sin(q_2+q_3)(\dot{q}_2+\dot{q}_3) - 2p_3l_2l_3\sin(q_3)\dot{q}_3 + (p_2+p_3)l_1l_2\sin(q_2)(\dot{q}_2+\dot{q}_1) + p_3l_1l_3\sin(q_2+q_3)(\dot{q}_2+\dot{q}_1+\dot{q}_3)$$

$$C_{22} = -2p_3l_2l_3\sin(q_3)\dot{q}_3$$

$$C_{23} = -p_3l_2l_3\sin(q_3)\dot{q}_3$$

$$C_{31} = -p_3l_1l_3\sin(q_2+q_3)(\dot{q}_2+\dot{q}_3) - p_3l_2l_3\sin(q_3)\dot{q}_3 + p_3l_1l_3\sin(q_2+q_3)(\dot{q}_2+\dot{q}_1+\dot{q}_3) + p_3l_2l_3\sin(q_2+q_3)(2\dot{q}_2+\dot{q}_1+\dot{q}_3)$$

$$C_{32} = p_3l_2l_3\sin(q_3)\dot{q}_2; C_{33} = 0;$$

$$G_1 = (p_1+p_2+p_3)gl_1sin(q_1) + (p_2+p_3)gl_2sin(q_1+q_2) + p_3gl_3sin(q_1+q_2+q_3)$$

$$G_2 = (p_2+p_3)gl_2sin(q_1+q_2) + p_3gl_3sin(q_1+q_2+q_3)$$

$$G_3 = p_3gl_3sin(q_1+q_2+q_3)$$

where p_1, p_2, p_3 are links masses; l_1, l_2, l_3 are links lengths; $g = 10(m/s^2)$.

The parameters of three link IRMs are given as follows:

$p_1 = 4.5\ (kg), p_2 = 3.2\ (kg), p_3 = 1.6\ (kg);$

$l_1 = 450\ (mm), l_2 = 340\ (mm), l_3 = 220\ (mm);$

The desired position trajectories of the three link industrial robot manipulators are chosen by:

$$\bar{q}_d = [q_{d1} \quad q_{d2} \quad q_{d3}]^T = [\sin(1.5t) \quad 0.5\sin(2t) \quad \sin(1.5t)]^T;$$

Initial positions of joints are $q_0 = \begin{bmatrix} 0.1 & 0 & -0.1 \end{bmatrix}^T$, and initial velocities of joints are $\dot{q}_0 = \begin{bmatrix} 0.0 & 0.0 & 0.0 \end{bmatrix}^T$.

External disturbances and friction force in this simulation are selected as following:

$$\tau_0 = \begin{bmatrix} 2\sin(t) \\ 2\sin(t) \\ 2\sin(t) \end{bmatrix}; F(\dot{q}) = \begin{bmatrix} 2sign(\dot{q}_1) \\ 2sign(\dot{q}_2) \\ 2sign(\dot{q}_3) \end{bmatrix}$$

The architecture of the ARNNs proposed controller can be characterized by n=5 nodes. The initial weight values of neural network are chosen as following:

$$\boldsymbol{W}_M = \begin{bmatrix} -1 & -0.5 & 0 & -0.5 & 1 \\ -1 & -0.5 & 0 & 0.5 & 1 \\ -1 & -0.5 & 0 & 0.5 & 1 \end{bmatrix}$$

$$\boldsymbol{W}_C = \begin{bmatrix} -1 & -0.5 & 0 & 0.5 & 1 \\ -1 & -0.5 & 0 & 0.5 & 1 \\ -1 & -0.5 & 0 & 0.5 & 1 \\ -1 & -0.5 & 0 & 0.5 & 1 \\ -1 & -0.5 & 0 & 0.5 & 1 \\ -1 & -0.5 & 0 & 0.5 & 1 \end{bmatrix}$$

$$\boldsymbol{W}_G = \begin{bmatrix} -1 & -0.5 & 0 & -0.5 & 1 \\ -1 & -0.5 & 0 & 0.5 & 1 \\ -1 & -0.5 & 0 & 0.5 & 1 \end{bmatrix}$$

$$\boldsymbol{W}_F = \begin{bmatrix} -1 & -0.5 & 0 & -0.5 & 1 \\ -1 & -0.5 & 0 & 0.5 & 1 \\ -1 & -0.5 & 0 & 0.5 & 1 \end{bmatrix}$$

The proposed controller parameter values are chosen as follows:

$\lambda_{q1} = diag(80, 80, 80); \lambda_{q2} = diag(60, 60, 60);$

$\lambda_{q2} = diag(40, 40, 40);$

$K_M = K_C = K_G = K_F = diag(15, 25, 25, 20);$

$\eta_M = \eta_C = \eta_G = \eta_F = 0.5;$

$\eta_P = diag(0.5, 0.07, 0.05);$

Here, Figure 4 are the results of the simulated comparison of the proposed ARNNs, and RBFNN [3] and Figure 5 are the results of the simulated comparison of the propsed ARNNs with disturbance and without disturbance. From the simulated results, we see that in all two cases the tracking position of RBFNN and the proposed intelligent controller are good. The tracking errors of ARNNs, and RBFNN are converged. However, the tracking errors of the proposed intelligent control system converge faster than the RBFNN systems. Moreover, from Figure 4 we can observe that, the control force of the proposed ARNNs is smoother and has a smaller oscillation than the RBFNN to achieve the requested level of performance when the tracking errors each the big value. It proves that all updated parameters in the dynamic structure ARNNs and the number of law nodes are adjusted, the approximation ability of the dynamics structure ARNNs is also better than the RBFNN systems. The robustness and control performance of the ARNNs scheme is still better than the RBFNN controller [3] under parameter variation and when the external disturbance.

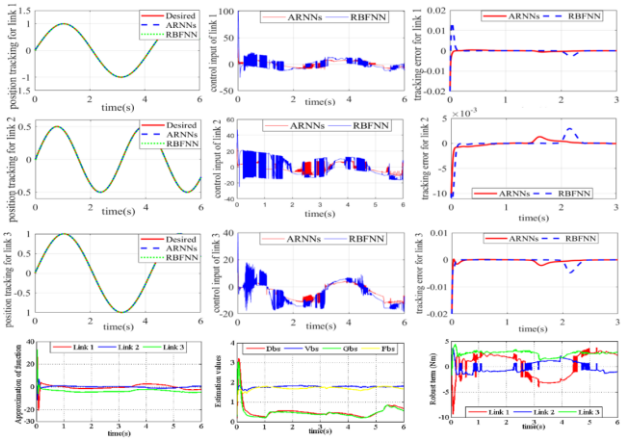

Figure 4. *The tracking error performances, control efforts, tracking errors of ARNNs, RBFNN, Robust term of ARNNs, and Approximation function of ARNNs*

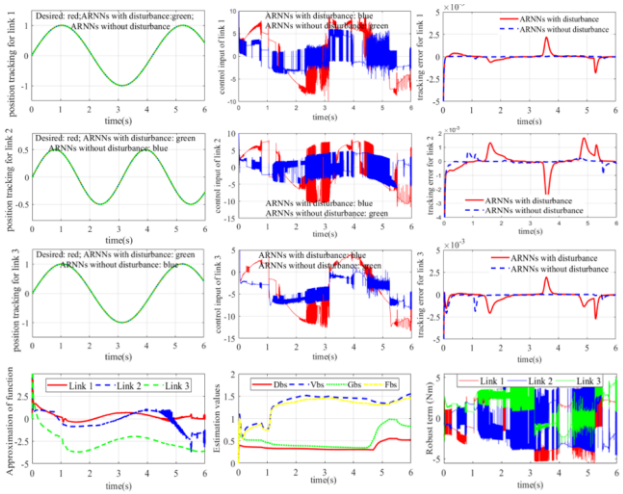

Figure 5. *The tracking error performances, control efforts, tracking errors of ARNNs with disturbance and without disturbance, Robust term of ARNNs, and Approximation function of ARNNs without disturbance*

5. Conclusions

In this studding, an adaptive robust backstepping controller combined with structure RBFNNs has been proposed. It has been also successfully implemented to control the joints of a three-link IRMs for achieving high precision position tracking by combining the advantages of RBFNNs, sliding mode robust term function, and adaptive

backstepping control technique. The difficulty to find approximate values of the unknown dynamic of IRMs has been solving by RBFNNs control. All the adaptive online trainings for the weights of the proposed intelligent control system are obtained by the Lyapunov theorem and trained online by an adaptive learning algorithm. From the Simulation results of three-links IRMs, we can find that the efficiency of the ARNNs proposed control is improved so much. The proposed ARNNs control system can also be applied to control for other systems, such as AC servo, MMR systems. This application could require further investigations.

REFERENCES

[1] Su, Y., Muller, P.C, and Zheng, C., "Global Asymptotic Saturated PID Control for Robot Manipulators", *IEEE Transactions on control systems technology*, vol 18, No 6, 2010, pp.1280- 1288.

[2] Baek, J., Jin, M., and Han, S., "A New Adaptive Sliding – Mode Control Scheme for Application to Robot Manipulators", *IEEE Transactions on industrial electronics*, Vol 27, 2016, pp. 525-536.

[3] Pham, V.C., Wang, Y.N., "Adaptive trajectory tracking neural network control with robust compensator for robot manipulator", *Neural Comput & Applic*, Vol, No 3, 2015, pp. 322-334.

[4] Kumar, V., Rana, K.P.S., "Nonlinear adaptive fractional order fuzzy PID control of a 2 – link planar rigid manipulator with payload", *Journal of the Franklin Institute*, 2017, pp. 993-1022.

[5] Chung, C.W., Chang, Y., "Backstepping control of multi – input non – linear systems", *IET Control Theory and Applications*, Vol 7, No 14, 2013, pp.1773-1779.

[6] Karagiannis, D., Astolfi, A., "Nonlinear adaptive control of systems in feedback from: An alternative to adaptive backstepping", *Systems & control letters*, Vol 57, 2008, pp. 733-739.

[7] Liu, J., Deng, H., Hu, C., Hua, Z., Chen, W., "Adaptive backstepping sliding mode control for 3-DOF permanent magnet spherical actuator", *Aerospace Science and Technology*, Vol 67, pp. 62-71.

[8] Montaseri, G., Yazdanpanah, M.J., "Adaptive control of uncertain nonlinear system using mized backstepping and Lyapunov redesign techniques", *Commun Nonlinear SCI Numer Simulat*, Vol 17, 2012, pp. 3367-3380.

[9] He, W., Chen, Y., and Yin, Z., "Adaptive Neural Network control of an Uncertain Robot with Full – State Constraints", *IEEE Transactions on Cybernetics*, Vol 46, No 3, 2016, pp. 620-629.

[10] Wang, M., Wang, A., "Dynamic Learning from Adaptive Neural Control of Robot Manipulators with Prescribed Performance", *IEEE Trans. Man, and Cybernetics: System*, Vol 48, No 8, 2017, pp.2244-2255.

[11] Kern, J., Jamett, M., Urrea, C., and Torres, H., "Development of a neural controller applied in a 5 DOF robot redundant", *IEEE Latin America Transactions*, Vol 12, No 2, 2014, pp.98-106.

[12] Ma, H., Wang, Z., Wang, D., Liu, D., Yan, P., and Wei, Q., "Neural – Network – Based Distributed Adaptive Robust Control for a Class of Nonlinear Multiagent Systems with time Delays and External Noises", *IEEE Transaction on systems, man, and cybernetics*, Vol 46, No 6, 2016, pp.750- 758.

[13] Rossomando, F.G., and Soria, C.M., "Design and Implementation of Adaptive Neural PID for Non Linear Dynamics in Mobile Robots", *IEEE Latin America Transactions*, Vol 13, No 4, 2015, pp.913-918.

[14] Sun, C., He, W., Ge, W., and Chang, C., "Adaptive Neural Network Control of Biped Robots", *IEEE Transaction on systems, man, and cybernetics: systems*, Vol 47, No 2, 2017, pp 315-326.

[15] Min, H., Lu, J., Xu, S., Duan, N., Chen, W., "Neural network – based output- feedback control for stochastic high – order non-linear time – delay systems with application to robot system", *IET Control Theorem & Applications*, Vol 11, No 10, 2017, pp.1578-1588.

[16] Chen, C.L.P., Wen, G.X., Liu, Y.J., and Wang, F.Y., "Adaptive Consensus Control for a Class of Nonlinear Multiagent Time- Delay Systems Using Neural Networks", *IEEE Transactions on neural networks and learning systems*, Vol 25, No 6, 2014, pp.1217-1226.

[17] He, W., David, O.A., Yang, C., Dawei, G., "Adaptive neural network control of a robotic manipulator with unknown backlash-like hysteresis", *IET Control Theory Appl*, Vol 11, No 4, pp.567-575.

[18] Slotine, J.J.E. and Li, W., "Applied Nonlinear control", *Hoboken, NJ: Prentice – Hall, 1991*.

[19] Vu, T. Y., Bui, V. H., Phung, T. V., "Thiết kế bộ điều khiển bền vững thích nghi trên cơ sở mạng nơ ron điều khiển cho robot công nghiệp", *Tạp chí Khoa học và Công nghệ - Đại học Đà Nẵng*, Vol. 18, No 11.1, 2020, pp 21-26.